Hindawi
Complexity
Volume 2019, Article ID 5125724, 12 pages
https://doi.org/10.1155/2019/5125724

Research Article

Traffic Model and On-Ramp Metering Strategy under Foggy Weather Conditions Using T-S Fuzzy Systems

Changle Sun and Hongyan Gao

College of Electrical Engineering and Automation, Shandong University of Science and Technology, Qingdao 266590, China

Correspondence should be addressed to Hongyan Gao; gaohongyan0107@163.com

Received 25 June 2019; Revised 15 September 2019; Accepted 19 November 2019; Published 9 December 2019

Guest Editor: Raúl Baños

Foggy weather seriously deteriorates the performance of freeway systems, particularly regarding traffic safety and efficiency. General macroscopic traffic models have difficulty reflecting the characteristics of a freeway under foggy weather conditions. In the present study, a macroscopic traffic model using a correction factor under foggy weather conditions is therefore proposed, which is regulated according to the different levels of visibility and curve radius of the freeway using the Takagi–Sugeno (T-S) model. Based on the proposed traffic model, a local ramp metering strategy with density correction under foggy weather conditions is proposed to improve traffic safety. The proposed local ramp metering strategy regulates the on-ramp flow using the T-S model according to the mainstream density, speed, and visibility. The correction factors are determined based on the parameters of the consequent part in the T-S model, which are optimized using the particle swarm optimization algorithm. The sum of the mean absolute percentage error of the mainstream traffic density and speed is used to evaluate the proposed traffic model. The real-time crash-risk prediction model, which reflects the degree of traffic safety, is used to evaluate the proposed local ramp metering strategy. Simulations using VISSIM and MATLAB show that the proposed traffic model is suitable under foggy weather conditions and that the proposed local ramp metering strategy achieves a better performance in reducing fog-related crashes.

1. Introduction

Foggy weather not only deepens the uncertainty, complexity, and randomness of freeway systems but also brings about a decrease in traffic efficiency and an increase in the number of crashes [1]. Fog-related crashes are mainly related to poor visibility and a large curve radius, which is the radius of a circularly curved section of a freeway [2].

Traffic management strategies for improving traffic safety and efficiency under foggy weather conditions can be divided into two types: advisory strategies and control strategies [3]. Advisory strategies using atmospheric and pavement data combined with the traffic flow and incident data can provide more timely and accurate freeway traffic information for travelers and thereby reduce fog-related crashes [4]. Dynamic traffic information can be automatically conveyed to travelers through dynamic message signs and freeway advisory announcements provided through a radio station. Control strategies can be divided into two types as well: speed management strategies and traffic flow management strategies. Regarding speed management, automatic visibility warning systems estimate a safe traffic speed for motorists based on the real-time visibility of the freeway as derived from visibility sensors to reduce fog-related crashes [5]. Real-time speed recommendations derived from visibility warning systems can be conveyed using an intelligent transportation system [6, 7]. A visibility warning system is widely used to ensure traffic safety under foggy weather conditions. Using six types of visibility sensors with forward-scatter technology and 25 closed circuit TV cameras, the Alabama Department of Transportation implemented a visibility warning system to reduce fog-related crashes [3]. The Utah Department of Transportation used an Adverse Visibility Information System Evaluation, which provides real-time speed recommendations for motorists, to reduce fog-related crashes [8, 9]. However, visibility warning systems have significant challenges in terms of cost and the application of appropriate sensor technologies.

In terms of traffic flow management, control strategies are applied to permit or restrict the traffic flow and regulate the freeway capacity. Ramp metering has been recognized as an effective and economic way to regulate mainstream freeway traffic flow at the cost of increasing or decreasing the on-ramp queue length [10]. Existing ramp metering strategies, including fixed-time and real-time ramp metering, have been used well. Based on historical traffic data, fixed-time ramp metering strategies may lead to freeway congestion or underutilization. Real-time ramp metering strategies including local responsive and coordinated ramp metering strategies regulate the mainstream traffic flow based on real-time traffic data. Local ramp metering strategies such as demand capacity, occupancy control, and Asservissement Linéaire d'Entrée Autoroutière (ALINEA) determine the on-ramp flow based on the real-time mainstream traffic conditions. Among them, ALINEA is the most typical type of ramp metering strategy owing to its closed-loop control [11]. Extended algorithms of ALINEA such as downstream-measurement-based adaptive ALINEA (AD-ALINEA), upstream-measurement-based adaptive ALINEA (AU-ALINEA) [12], and proportional-integral extension of ALINEA (PI-ALINEA) [13] have recently been proposed. In addition, intelligent control algorithms such as iterative learning control [14–16], fuzzy logic control (FLC), neural network control [17], and a reinforcement learning control algorithm [18] are used in local ramp metering. Coordinated ramp metering strategies such as METALINE, FLOW, the Zone algorithm, Helper, and SWARM aim at improving the network-wide traffic efficiency of freeways by making full use of all on-ramps. However, the complexity and cost of coordinated ramp metering are much higher than those of local ramp metering [19].

A freeway system is an interconnected nonlinear system that can be represented using a set of linear state equations by applying a fuzzy model. Therefore, FLC appears to be more suitable for ramp metering than an analytic control algorithm. A fuzzy logic controller based on six input variables and three output variables was proposed for ramp metering, which took into account the upstream and downstream traffic states and the length of the on-ramp queue [20]. Experimentally, the fuzzy controller proved its superior performance in reducing congestion and dealing with traffic incidents. In addition, a T-S-type fuzzy controller based on the mainstream density, speed, and queue length applied as inputs and the desired mainstream density applied as the output was proposed [21]. The proposed T-S-type fuzzy controller implements an optimal ramp metering according to the different traffic states using the PSO algorithm. The self-adjusted fuzzy ramp metering strategy based on the correction factor was proposed [21]. The fuzzy control rules of the proposed self-adjusted fuzzy ramp metering strategy are replaced with correction factors. The proposed correction factors simplify the rule definitions of the three-dimensional fuzzy controller. Based on the fuzzy logic algorithm, many different control strategies such as a genetic-fuzzy algorithm [22] and a genetic-fuzzy algorithm with the optimization algorithm [23] have been proposed. Moreover, a ramp metering strategy based on the fuzzy logic algorithm achieves a good robustness and rapid response to traffic demand [24].

Although studies on local ramp metering under normal weather conditions have been exploited well, few studies have been conducted on local ramp metering under foggy weather conditions. In this study, a macroscopic traffic model based on a model correction factor (c_m) under foggy weather conditions is proposed using the T-S model. The traffic model is regulated using the T-S model according to the different degrees of visibility and the curve radius of the freeway. Freeway traffic data derived from the VISSIM simulator are used for traffic modelling under foggy weather conditions. The sum of the mean absolute percentage error based on the mainstream traffic density and speed is used to evaluate the proposed traffic model. The traffic model parameters are optimized using the PSO algorithm. The proposed traffic model is simulated in MATLAB.

Based on the proposed macroscopic traffic model, a local ramp metering strategy based on a density correction factor (c_d) under foggy weather conditions is proposed. Based on a T-S-type FLC, the proposed local ramp metering strategy regulates the on-ramp flow according to the mainstream density, mainstream speed, and visibility. A real-time crash-risk prediction model reflecting the level of safety of the freeway traffic is used to evaluate the proposed local ramp metering strategy. The parameters of the proposed ramp metering strategy are also optimized using the PSO algorithm, and the proposed local ramp metering strategy is simulated in MATLAB.

2. Macroscopic Traffic Model under Foggy Weather Conditions

2.1. T-S-Type Fuzzy Theory. In this study, the T-S model is adopted for use as a macroscopic traffic model and for local ramp metering under foggy weather conditions. For a T-S-type fuzzy controller, x_m is denoted as the m-th input variable, with $m = 1, \ldots, M$, where M is the number of input variables; in addition, $A^i(x_m)$ is denoted as the input fuzzy subset of the input variable x_m corresponding to the i-th fuzzy rule, in which $i = 1, \ldots, N$, where N is the number of fuzzy rules. The i-th fuzzy rule is expressed in the IF-THEN form as follows:

$$\underbrace{\text{IF } x_1 \text{ is } A^i(x_1) \text{ AND } x_2 \text{ is } A^i(x_2) \cdots \text{AND } x_M \text{ is } A^i(x_M)}_{\text{antecedent part}}$$
$$\underbrace{\text{THEN } y^i = p_0^i + p_1^i x_1 + \cdots + p_M^i x_M}_{\text{consequent part}}, \tag{1}$$

where p_l^i is a constant parameter of the consequent part related to the i-th fuzzy rule, in which $l = 0, 1, \ldots, M$, and y^i denotes the output value corresponding to this rule.

In addition, $\mu^i(x_m)$ denotes the membership value of the input variable x_m corresponding to the linguistic variable

$A^i(x_m)$, and μ^i refers to the membership value of the i-th fuzzy rule, which is calculated as follows:

$$\begin{aligned} \mu^i &= \min\left(\mu^i(x_1), \mu^i(x_2), \ldots, \mu^i(x_M)\right) \\ \text{or } \mu^i &= \mu^i(x_1) * \mu^i(x_2) * \cdots * \mu^i(x_M). \end{aligned} \tag{2}$$

The final output of the T-S model is expressed as follows:

$$y = \frac{\sum_i \mu^i y^i}{\sum_i \mu^i}. \tag{3}$$

2.2. Macroscopic Traffic Model with Correction Factor under Foggy Weather Conditions. Considering such factors as the topography and construction costs in the design of a freeway plane alignment, circular curved sections are unavoidable and are applied as a main linear section of a freeway. Owing to the particularity of its linear conditions and the complexity of driving behaviors, such sections have become areas with a high incidence of traffic accidents. The freeway friction coefficient and visibility are reduced under foggy weather conditions, adding to the complexity of driving behaviors on curved sections. The curve radius is the main characteristic of a circular curved section of a freeway, and the crash risk will increase with a decrease in the curve radius. The freeway visibility and curve radius are two of the most critical factors affecting the traffic model applied under foggy weather conditions. METANET [25] is a well-known macroscopic traffic model. However, it has difficulty reflecting freeway characteristics under foggy weather. Therefore, in this study, a traffic model applied under foggy weather conditions that introduces a model correction factor (c_m) into the METANET traffic model is proposed. This model correction factor can reflect the effects of foggy weather on a freeway because the factor is regulated according to the different levels of visibility and the curve radius of the freeway. The model correction factor is directly determined using the T-S model. The proposed traffic model is expressed as follows:

$$\rho_i(k+1) = c_m \cdot \left(\rho_i(k) + \frac{T}{\Delta_i}\left[q_{i-1}(k) - q_i(k) + u_i(k)\right]\right), \tag{4}$$

$$q_i(k) = \rho_i(k) \cdot v_i(k) \cdot \lambda_i, \tag{5}$$

$$\begin{aligned} v_i(k+1) = c_m \cdot \Bigg(& v_i(k) + \frac{T}{\tau}\left[V(\rho_i(k)) - v_i(k)\right] \\ & + \frac{T}{\Delta_i} v_i(k)\left[v_{i-1}(k) - v_i(k)\right] \\ & - \frac{\gamma T}{\tau \Delta_i} \frac{\rho_{i+1}(k) - \rho_i(k)}{\rho_i(k) + \theta} \Bigg), \end{aligned} \tag{6}$$

$$V(\rho_i(k)) = v_f \cdot \left[1 - \left(\frac{\rho_i(k)}{\rho_{\text{jam}}}\right)^{\delta}\right]^m, \tag{7}$$

where T is the length of the time step; k indicates the time step $t = kT$, where $k = 1, \ldots, \lambda_i$ denotes the number of lanes in the segment i; $v_i(k)$ and $\rho_i(k)$ are the average speed and average mainstream density in the segment i at the time step kT, respectively; $q_i(k)$ represents the mainstream flow through the segment i entering the next segment during the time step kT; $u_i(k)$ represents the on-ramp metering flow entering the segment i at the time step kT; the notations v_f, ρ_{jam}, Δ_i, and $V(\rho_i(k))$ represent the free-flow speed, the jam density, the length of the segment i, and the static speed in the segment i at the time step kT, respectively; m, γ, τ, δ, and θ are global parameters reflecting the freeway characteristics; and c_m denotes the model correction factor. Equations (4)–(7) are for determining the conservation, traffic parameter relationship, dynamic mean speed, and static speed-density relationship, respectively.

2.3. Model Correction Factor Regulation Based on T-S Model. The visibility and curve radius are the two most important factors affecting freeway traffic under the foggy weather condition. Thus, in this study, the freeway visibility and curve radius are applied as input variables of the T-S model, and the model correction factor is applied as the output variable. The freeway visibility and curve radius can be obtained from a freeway information system. The freeway visibility and curve radius at the time step kT are denoted as $r(k)$ and $b(k)$, respectively. Assume that $A(r)$ and $A(b)$ are the input fuzzy sets of the input variables $r(k)$ and $b(k)$, respectively. Two input fuzzy subsets are defined for each input fuzzy set. The normalized domain of the input fuzzy sets and the input variables is $[-1, 1]$. It is assumed that the actual physical domains of the visibility and radius curve are $[r_1, r_2]$ and $[b_1, b_2]$, respectively. The mean values of r_m and b_m and the scaling factors K_r and K_b are used to transform the physical domains $[r_1, r_2]$ and $[b_1, b_2]$ into the normalized domains $[-1, 1]$ and $[-1, 1]$, respectively, the mathematical formulas of which are as follows:

$$\begin{aligned} r_m &= \frac{r_1 + r_2}{2}, \\ b_m &= \frac{b_1 + b_2}{2}, \\ K_r &= \frac{1}{(r_2 - r_m)}, \\ K_b &= \frac{1}{(b_2 - b_m)}. \end{aligned} \tag{8}$$

Thus, the measured values $r(k)$ and $b(k)$ can be transformed into the normalized domain using the appropriate scaling factors as follows:

$$\begin{aligned} A(r) &= K_r \cdot (r(k) - r_m), \\ A(b) &= K_b \cdot (b(k) - b_m). \end{aligned} \tag{9}$$

The membership function of normalized input fuzzy sets described using a trapezoidal function [26] is as shown in Figure 1.

There are four different combinations of input variables in the fuzzy rules, as summarized in Table 1.

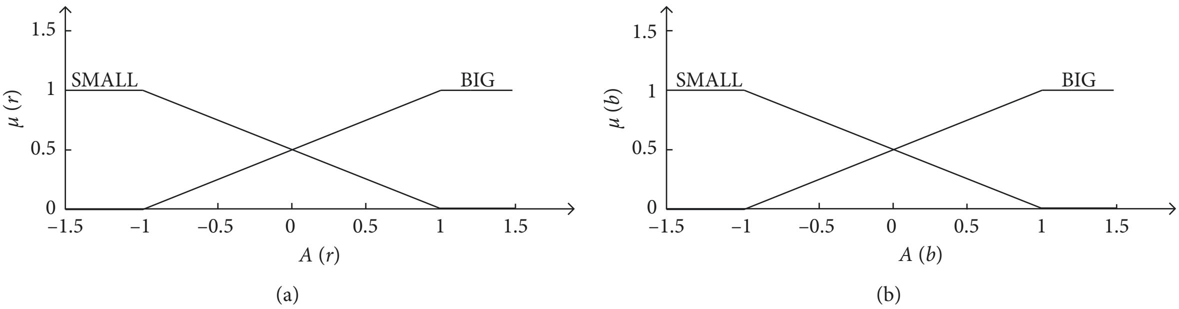

Figure 1: Membership functions of (a) visibility and (b) curve radius.

Table 1: Combinations of input variables in fuzzy rules.

i	$A(r)$	$A(b)$
1	SMALL	BIG
2	SMALL	SMALL
3	BIG	SMALL
4	BIG	BIG

An example of a fuzzy rule is expressed in the IF-THEN form as follows:

$$\underbrace{\text{IF } r \text{ is BIG AND } b \text{ is SMALL}}_{\text{antecedent part}} \\ \underbrace{\text{THEN } c_m^i = \beta_0^i + \beta_1^i r + \beta_2^i b,}_{\text{consequent part}} \tag{10}$$

where β_j^i, in which $j = 0, 1, 2$, is a constant parameter of the consequent part corresponding to the i-th fuzzy rule and c_m^i denotes the output value corresponding to the i-th fuzzy rule.

According to equations (1)–(3), the model correction factor (c_m) is calculated as follows:

$$c_m = \frac{\sum_i \mu^i c_m^i}{\sum_i \mu^i}. \tag{11}$$

The T-S model of the model correction factor contains four fuzzy rules, and each fuzzy rule has three parameters to be regulated. Thus, the T-S model regulates a total of 12 parameters. Including v_f, τ, ρ_{jam}, m, γ, θ, and δ, there are a total of 19 parameters to be regulated in the proposed traffic model. The performance of the T-S model depends on the structure and parameter identification. However, in this study, the performance of the T-S model is merely related to the parameters of the consequent part because the input fuzzy sets are predefined. Therefore, to minimize the performance objective, the problem of traffic modelling under foggy weather conditions is equivalent to seeking the optimal values of the 19 parameters. The PSO algorithm is adopted to optimize these parameters.

2.4. Parameter Regulation Based on PSO. As a swarm intelligence algorithm, PSO is inspired by the search strategy applied in the foraging behaviors of organisms such as flocking bird [27]. The PSO algorithm is based on a population iterative search. For the parameter optimization, each particle denotes a set of candidate solutions. Each particle includes the position and velocity, which determine its direction and distance of flight, as well as the fitness value calculated using a fitness function. During the particle search process, each particle can update its position in a better direction by tracking the individual and global best positions. If the number of iterations reaches the maximum, the global best position of the particle swarm is the optimal solution. During each iteration, each particle updates its velocity and position by tracking the individual and global best positions as follows [28]:

$$\begin{aligned} v_i^{j+1} &= w v_i^j + c_1 r_1 \left(p_i^j - x_i^j\right) + c_2 r_2 \left(p_g^j - x_i^j\right), \\ x_i^{j+1} &= x_i^j + v_i^{j+1}, \end{aligned} \tag{12}$$

where i refers to the index of the particle, j represents the index of the iteration, v_i^j denotes the velocity of the i-th particle during the j-th iteration, x_i^j denotes the position of the i-th particle during the j-th iteration, p_i^j is the individual best position of the i-th particle during the j-th iteration, p_g^j is the global best position of the particle swarm during the j-th iteration, w is the inertia weight, c_1 and c_2 are learning factors regulating the attraction of the individual and global best positions to the particle, and r_1 and r_2 are random values within the range of zero to 1.

During the application of the PSO algorithm, the fitness function is used to evaluate the effectiveness of the parameter optimization during the k-th iteration. The sum of the mean absolute percentage error of the mainstream traffic density and speed is used for the fitness function. The fitness function is expressed as follows:

$$J = 0.5 \sum_{1 \le k \le K} \left\{ \frac{\left|\rho_o(k) - \rho_i(k)\right|}{\rho_o(k)} + \frac{\left|v_o(k) - v_i(k)\right|}{v_o(k)} \right\}, \tag{13}$$

where k indicates the time step $t = kT$, where $k = 1, 2, \ldots, K$ is the total time period; $\rho_o(k)$ and $\rho_i(k)$ are the actual mainstream density and the density derived from the proposed traffic model at the time step kT, respectively; and $v_o(k)$ and $v_i(k)$ are the actual mainstream speed and the speed derived from the proposed traffic model at the time step kT, respectively; in addition, the data on $\rho_o(k)$ and $v_o(k)$ under foggy weather conditions can be obtained from a freeway information system.

The mainstream traffic flow is a product of the mainstream traffic density and speed, and thus, the mainstream flow is indirectly taken into account through the fitness function. It is known that the speed, density, and flow are considered to be explanatory variables of the freeway traffic model. Therefore, the fitness function, which includes the mainstream speed, density, and flow, represents a comprehensive assessment of the proposed traffic model.

The implementation steps of the PSO algorithm are divided into two parts: initialization and iteration.

2.4.1. Initialization Part

Step 1. Set the particle swarm size as 100, the number of particle dimensions as 19, the maximum number of iterations as 300, both c_1 and c_2 as 2, and the inertia weight w as 0.8.

Step 2. Initialize the position and velocity vectors for each particle randomly while taking into account the particle limits.

Step 3. Input the traffic data on the flow, speed, and density.

Step 4. Randomly set the initial solution of each particle, and initialize the individual and global best positions.

2.4.2. Iteration Part

Step 1. Calculate the fitness value of each particle according to equations (4)–(7) and (12).

Step 2. Determine the individual and global best positions for the i-th particle at the j-th iteration, and if the fitness value is smaller than the previous fitness value, let the individual best position $p_i^j = x_i^j$; otherwise, the individual best position p_i^j remains unchanged. In addition, if the individual best position p_i^j is smaller than the global best position p_g^j, let $p_g^j = p_i^j$; otherwise, the global best position p_g^j remains unchanged.

Step 3. Update the velocity and position of each particle according to equation (11).

Step 4. Repeat the iteration part until the maximum number of iterations is satisfied.

3. Local Ramp Metering under Foggy Weather Conditions

During the past several decades, studies on local ramp metering under normal weather conditions have been well exploited. However, the problem of local ramp metering under foggy weather conditions has been rarely studied. Because of traffic safety, on-ramps are typically closed under foggy weather conditions. The consequence of closing an on-ramp is not only a reduction in the mainstream traffic flow but also a decrease in the traffic efficiency. Therefore, improving the freeway traffic efficiency during foggy weather on the basis of ensuring traffic safety is a popular area of study. Owing to the complexity of foggy weather conditions, the desired density varies from moment to moment, which cannot be properly solved using PI-ALINEA. Thus, the application of local ramp metering under foggy weather conditions is proposed.

A ramp metering strategy similar to PI-ALINEA is applied in the present paper. PI-ALINEA is expressed as follows:

$$u(k+1) = u(k) - K_P[\rho(k) - \rho(k-1)] + K_R[\rho_d - \rho(k)], \tag{14}$$

where K_P and K_R are the gain factors for the proportional and integral terms, respectively.

The proposed local ramp metering strategy based on the density correction factor (c_d) can regulate the on-ramp flow according to the freeway traffic state. In addition, the density correction factor (c_d) is directly determined using the T-S model. The proposed local ramp metering strategy based on the density correction factor (c_d) can be expressed as follows:

$$u(k+1) = u(k) - K_P[\rho(k) - \rho(k-1)] + K_R[\rho_d - \rho(k)], \tag{15}$$

$$\rho_d = \rho_p \cdot c_d, \tag{16}$$

where K_P and K_R are the gain factors for the proportional and integral terms, respectively; ρ_p is the predefined density value; and c_d represents the density correction factor.

The mainstream traffic density (ρ), speed (v), and visibility (r) of the freeway are three key factors affecting the traffic safety under foggy weather conditions. Thus, this paper sets the mainstream traffic density (ρ), speed (v), and visibility (r) as input variables of the T-S model and the density correction factor (c_d) as the output variable. Assume that $A(\rho)$, $A(v)$, and $A(r)$ are input fuzzy sets of the mainstream density, speed, and visibility, respectively. Two fuzzy subsets are defined for each input fuzzy set. The normalized domains of the input fuzzy sets and input variables are all $[-1, 1]$. Assume that the actual physical domains of the visibility, speed, and visibility are $[\rho_1, \rho_2]$, $[v_1, v_2]$, and $[r_1, r_2]$, respectively. The mean values of ρ_m, v_m, and r_m and the scaling factors K_ρ, K_v, and K_r transform the physical domains $[\rho_1, \rho_2]$, $[v_1, v_2]$, and $[r_1, r_2]$ into the normalized domains $[-1, 1]$, $[-1, 1]$, and $[-1, 1]$, respectively, the mathematical formulas of which are as follows:

$$\begin{aligned}
\rho_m &= \frac{\rho_1 + \rho_2}{2}, \\
v_m &= \frac{v_1 + v_2}{2}, \\
r_m &= \frac{r_1 + r_2}{2}, \\
K_\rho &= \frac{1}{\rho_2 - \rho_m}, \\
K_v &= \frac{1}{v_2 - v_m}, \\
K_r &= \frac{1}{r_2 - r_m}.
\end{aligned} \tag{17}$$

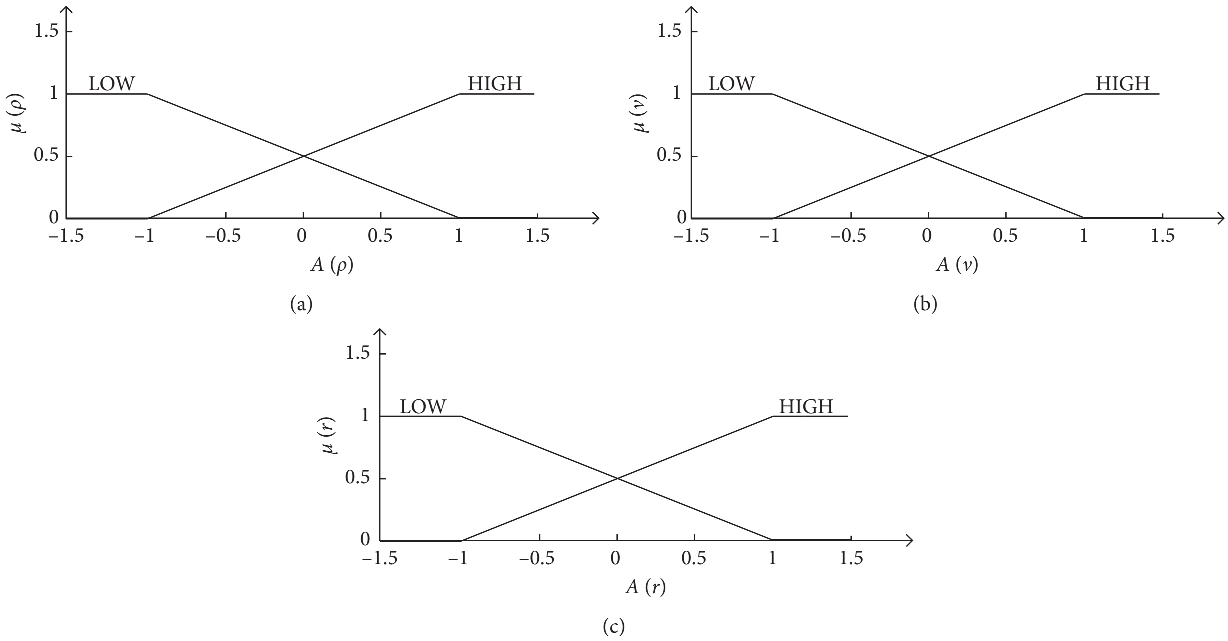

Figure 2: Membership functions of (a) mainstream density, (b) mainstream speed, and (c) visibility.

Table 2: Combinations of input variables used in fuzzy rules.

i	$A(\rho)$	$A(v)$	$A(r)$
1	HIGH	LOW	HIGH
2	HIGH	LOW	LOW
3	LOW	HIGH	HIGH
4	LOW	HIGH	LOW

Thus, the measured values $r(k)$ and $b(k)$ can be transformed into the normalized domain as follows:

$$\begin{aligned} A(\rho) &= K_\rho \cdot \left(\rho(k) - \rho_m\right), \\ A(v) &= K_v \cdot \left(v(k) - v_m\right), \\ A(r) &= K_r \cdot \left(r(k) - r_m\right). \end{aligned} \tag{18}$$

The membership function of the normalized input fuzzy sets described using a trapezoidal function is shown in Figure 2.

Owing to dynamic characteristics of a traffic flow, when the mainstream traffic density is high, the mainstream traffic speed should be low. Therefore, four different combinations of input variables are applied in the fuzzy rules, as summarized in Table 2.

For example, the i-th fuzzy rule is expressed as follows:

$$\begin{aligned} &\underbrace{\text{IF } \rho \text{ is HIGH AND } v \text{ is LOW AND } r \text{ is HIGH}}_{\text{antecedent part}} \\ &\underbrace{\text{THEN } c_d^i = o_0^i + o_1^i\rho + o_2^i v + o_3^i r}_{\text{consequent part}}, \end{aligned} \tag{19}$$

where o_j^i, in which $j = 0, 1, 2, 3$, is a constant parameter of the consequent part corresponding to the i-th fuzzy rule and c_d^i denotes the output value corresponding to the i-th fuzzy rule.

According to equations (1)–(3), the density correction factor (c_d) can be calculated as follows:

$$c_d = \frac{\sum_i \mu^i c_d^i}{\sum_i \mu^i}. \tag{20}$$

According to equations (15) and (18), the desired density can be calculated as follows:

$$\rho_d = \rho_p \cdot \left(\frac{\sum_i \mu^i c_d^i}{\sum_i \mu^i}\right). \tag{21}$$

The T-S model of the density correction factor contains four fuzzy rules, each of which has four parameters to be regulated. Thus, the T-S model has 16 parameters to regulate in the proposed local ramp metering strategy. The PSO algorithm is used to optimize these 16 parameters.

The principle and implementation steps of the PSO algorithm are described in Section 2.4. The determined difference is the fitness function. Freeway traffic safety during foggy weather conditions is the primary control target. Thus, the real-time crash-risk prediction model, which reflects the traffic safety, is used as the fitness function to evaluate the proposed local ramp metering. The real-time crash-risk prediction model is actually described as a logistic regression function of the freeway traffic variables and regulates the model parameters using the actual freeway traffic incident data. The real-time crash-risk prediction model [29] is calculated as follows:

$$\overline{V}_U(t - \Delta T, t) = \frac{\sum_{\lambda=1}^{\lambda_i} \sum_{n=1}^{N_1} V_U^\lambda(t_n - \Delta t, t_n)}{\lambda_i \cdot N_1}, \tag{22}$$

$$\overline{V}_D(t - \Delta T, t) = \frac{\sum_{\lambda=1}^{\lambda_i} \sum_{n=1}^{N_1} V_D^\lambda(t_n - \Delta t, t_n)}{\lambda_i \cdot N_1}, \tag{23}$$

$$\overline{O}_U(t - \Delta T, t) = \frac{\sum_{\lambda=1}^{\lambda_i} \sum_{n=1}^{N_1} O_D^\lambda(t_n - \Delta t, t_n)}{\lambda_i \cdot N_1}, \tag{24}$$

$$\text{RCRI} = \frac{\left[\overline{V}_U(t-\Delta T,t) - \overline{V}_D(t-\Delta T,t)\right]\cdot \overline{O}_U(t-\Delta T,t)}{1-\overline{O}_U(t-\Delta T,t)}, \tag{25}$$

$$\sigma(O_U) = \sqrt{\frac{\sum_{\lambda=1}^{\lambda_i}\sum_{n=1}^{N_1}\left[O_U^{\lambda}(t_n-\Delta t,t_n) - \overline{O}_U(t-\Delta T,t)\right]^2}{\lambda_i\cdot N_1}}, \tag{26}$$

$$\sigma(O_D) = \sqrt{\frac{\sum_{\lambda=1}^{\lambda_i}\sum_{n=1}^{N_1}\left[O_D^{\lambda}(t_n-\Delta t,t_n) - \overline{O}_D(t-\Delta T,t)\right]^2}{\lambda_i\cdot N_1}}, \tag{27}$$

$$\begin{aligned}\text{Logit}(P(Y=1)) = \alpha_1 + \alpha_2\cdot \text{RCRI} + \alpha_3\cdot\sigma(O_U)\\ + \alpha_4\cdot\sigma(O_D),\end{aligned} \tag{28}$$

$$P(Y=1) = \frac{\exp(\alpha_1+\alpha_2\cdot\text{RCRI}+\alpha_3\cdot\sigma(O_U)+\alpha_4\cdot\sigma(O_D))}{1+\exp(\alpha_1+\alpha_2\cdot\text{RCRI}+\alpha_3\cdot\sigma(O_U)+\alpha_4\cdot\sigma(O_D))}, \tag{29}$$

where $\overline{V}_U(t-\Delta T,t)$ and $\overline{V}_D(t-\Delta T,t)$ are the average speed in the upstream and downstream segments during the time period ΔT, respectively; $\overline{O}_U(t-\Delta T,t)$ denotes the average occupancy in the upstream segment during the time period ΔT; RCRI represents the rear-end collision risk induced by kinematic waves; and $V_U^{\lambda}(t_n-\Delta t,t_n)$ and $V_D^{\lambda}(t_n-\Delta t,t_n)$ are the average speed of the λ-th lane in the upstream and downstream segments during the time interval Δt, respectively. In addition, $O_U^{\lambda}(t_n-\Delta t,t_n)$ is the average occupancy of the λ-th lane in the upstream segment during the time interval Δt; $\sigma(O_U)$ and $\sigma(O_D)$ are the standard deviation of the occupancy in the upstream and downstream segments during the time period ΔT, respectively; λ_i is the number of lanes in the segment i; N_1 is the number of time intervals in a single time period ($N_1=\Delta T/\Delta t$); $P(Y=1)$ is the probability of a crash; and α_1, α_2, α_3, and α_4 are constant parameters.

In this study, the performance of the T-S model is simply related to the parameters of the consequent part because the input fuzzy sets are predefined. Therefore, the problem of local ramp metering under foggy weather conditions is equivalent to seeking the optimal values of the 16 parameters to minimize the performance objective. The configuration parameters of the PSO algorithm used in the proposed local ramp metering strategy are listed in Table 3.

Table 3: Combinations of input variables in fuzzy rules.

Parameter	Value
N_2 (swarm size)	100
K	300
w	0.8
c_1	2.0
c_2	2.0

4. Simulation Experiment and Analysis

4.1. Simulation of Traffic Model under Foggy Weather Conditions

4.1.1. Experimental Setup. The hypothetical freeway stretch is divided into five segments with a length of Δx_i, namely, $\Delta x_1 = 643$ m, $\Delta x_2 = 643$ m, $\Delta x_3 = 643$ m, $\Delta x_4 = 643$ m, and $\Delta x_5 = 643$ m. The hypothetical freeway stretch has two lanes and two on-ramps. The lengths of on-ramps $R1$ and $R2$ are both 400 m. The hypothetical freeway stretch is shown in Figure 3.

Segment 4 is used for traffic modelling under foggy weather conditions. The freeway traffic data under such conditions derived from VISSIM with time intervals of 5 min are used as inputs for the traffic modelling, as shown in Figure 4. The demand (Q_3) of segment 3 from detector 4 and demand (d_2) of on-ramp R2 from detector 8 are shown in Figure 4(a). The units of the segment 3 demand (Q_3) and on-ramp $R2$ demand (d_2) are both the hourly flow. The average speed (V_3) of segment 3 from detector 4 and the density (ρ_5) of segment 5 from detector 6 are shown in Figures 4(b) and 4(c), respectively. The experiment simulates the freeway traffic from 1 : 00 am to 23 : 40 pm with a simulation time step of 10 s.

The higher the fog concentration, the lower the visibility. To analyze the effects of foggy weather on the freeway conditions, the traffic data on the density and speed in segment 4 are sampled from VISSIM under different freeway visibility conditions, as shown in Figure 5. As Figure 5(a) indicates, the desired density of the freeway decreases with the elevated concentration of fog. As shown in Figure 5(b), the speed fluctuation is greater with the increase in fog concentration. Therefore, the freeway traffic safety and efficiency decrease with the elevated concentration of fog. The influence of foggy weather on the traffic model is mainly in terms of density and speed.

The proposed traffic model was simulated using the traffic data under foggy weather conditions as derived from VISSIM. Two cases were simulated with a visibility of $r = 150$ m and a curve radius of $b = 1{,}500$ m. For case 1, one model correction factor is used for the traffic model under foggy weather conditions. For case 2, two model correction factors are used for the traffic model under such conditions. The parameters used for the proposed traffic model are set as follows: initial speed $v(1) = 97$ km/h and initial density $\rho(1) = 0.735$ veh/km/ln, where the actual physical domains of the visibility and curve radius in the traffic model are [100 m, 200 m] and [500 m, 1,500 m], respectively. According to equation (8), mean values of $r_m = 100$ m and $b_m = 1000$ m and scaling factors of $K_r = 0.02$ and $K_b = 0.002$ are used.

4.1.2. Simulation Results and Analysis. As shown in Figure 6, one model correction factor (c_m) is applied to the mainstream traffic density and velocity. The fitness value is used to evaluate the performance of the proposed traffic model. According to equation (12), the fitness value of the traffic model with one model correction factor (c_m) is 5.96%. As

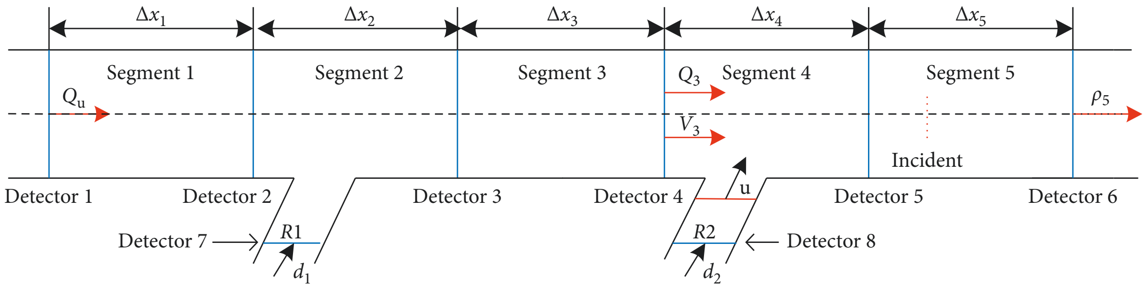

FIGURE 3: Hypothetical freeway stretch.

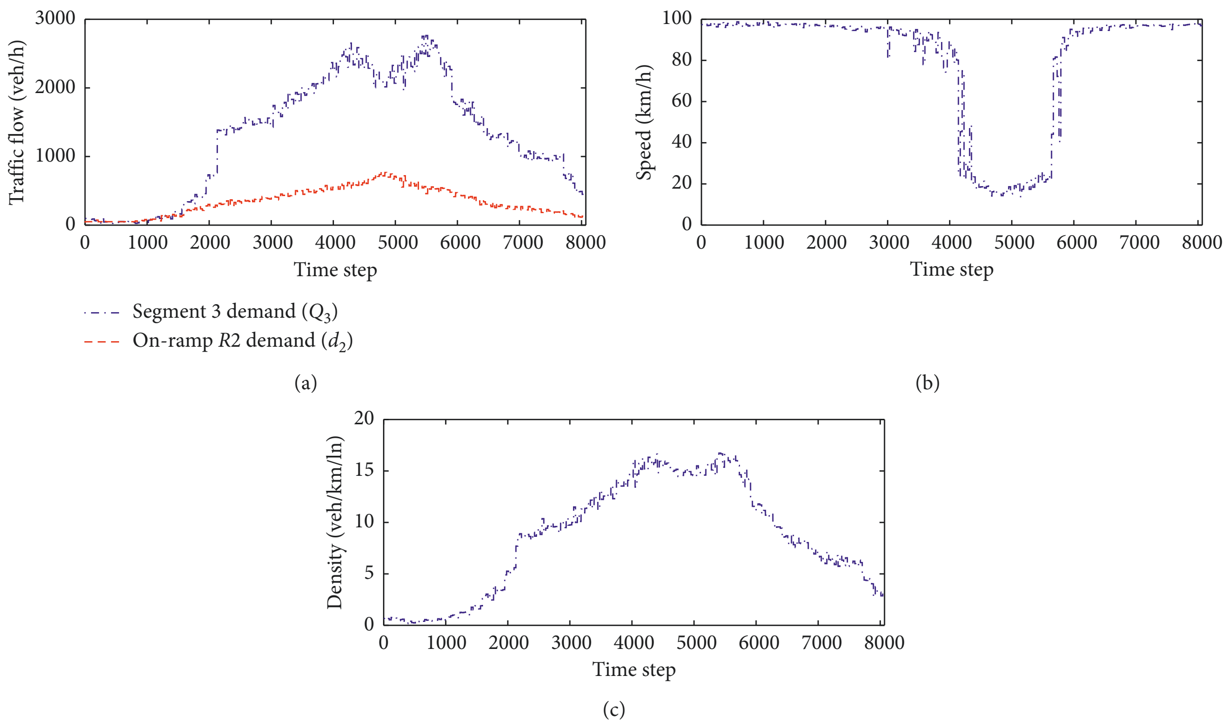

FIGURE 4: (a) Demands of segment 3 and on-ramp $R2$, (b) average speed of segment 3, and (c) average density of segment 5.

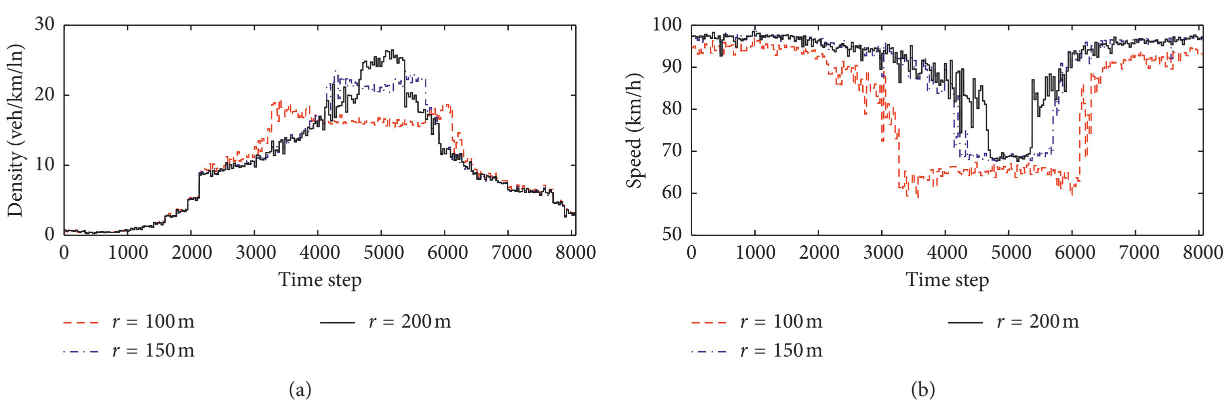

FIGURE 5: (a) Mainstream density and (b) mainstream speed under different foggy weather conditions.

indicated in Figure 7, two model correction factors c_{m1} and c_{m2} are applied to the mainstream traffic density and speed, respectively. The fitness value of the traffic model with two model correction factors is 6.22%. Clearly, the traffic model with one model correction factor achieves a better performance than that with two factors.

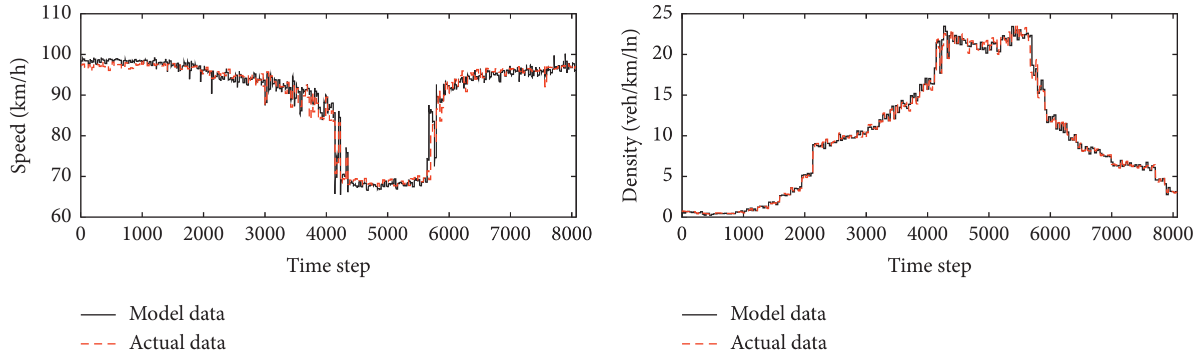

(a) (b)

FIGURE 6: (a) Model speed and actual speed and (b) model density and actual density of case 1.

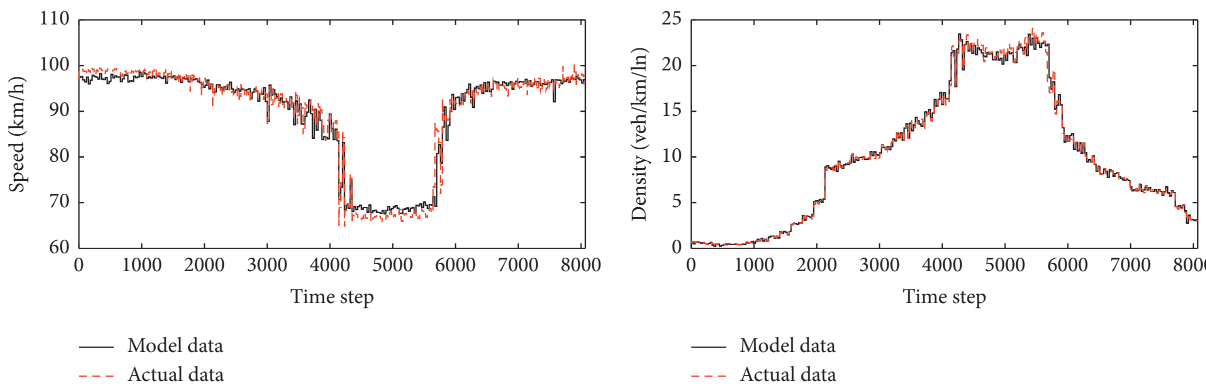

(a) (b)

FIGURE 7: (a) Model speed and actual speed and (b) model density and actual density of case 2.

The 19 parameters used in the traffic model with one model correction factor through the PSO algorithm are regulated as follows: $\rho_{\text{jam}} = 88.9889$ veh/km/ln, $v_f = 99.1510$ km/h, $\tau = 18$ s, $\gamma = 45.5616\,\text{km}^2/\text{h}$, $\theta = 11.0836$ veh/km, $m = 1$, $\delta = 1.1861$, $f_1 = 0.7631$, $f_2 = 0.5976$, $f_3 = 0.2099$, $f_4 = 0.6452$, $f_5 = 0.1955$, $f_6 = 0.3291$, $f_7 = 0.7095$, $f_8 = 0.1745$, $f_9 = 0.3159$, $f_{10} = 0.0034$, $f_{11} = 0.0535$, and $f_{12} = 0.3515$. The model correction factor (c_m) is calculated from parameters f_1 through f_{12}, and the value of 0.99 is obtained.

4.2. Simulation of the Proposed Ramp Metering Strategy under Foggy Weather Conditions

4.2.1. Experimental Setup. Freeway traffic data with time intervals of 10 s, such as for the upstream demand (Q_u) and on-ramp demand (d_1 and d_2), are employed as the input data of the local ramp metering under foggy weather conditions, as shown in Figure 8. The units of upstream demand (Q_u), on-ramp $R1$ demand (d_1), and on-ramp $R2$ demand (d_2) are all hourly flow. The simulation time step is 10 s, and the control time step is 30 s. Owing to the low on-ramp flow, a no-control measure is used for on-ramp $R1$. On-ramp $R2$ is controlled using PI-ALINEA and the proposed ramp metering strategy. PI-ALINEA is described in equation (13). The simulations are carried out using a visibility of 150 m and a curve radius of 1,200 m. The parameters used for the traffic modelling are set as follows: initial upstream demand $Q_u(1) = 2730$ veh/h, initial on-ramp $R1$ demand $d_1(1) = 181$ veh/h, initial on-ramp $R2$ demand $d_2(1) = 301$ veh/h, maximum ramp metering flow $u_{\max} = 1000$ veh/h, and minimum ramp metering $u_{\min} = 100$ veh/h, and the actual

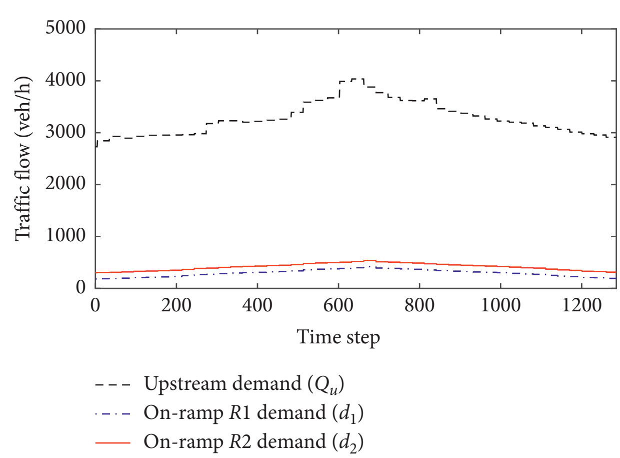

FIGURE 8: Traffic demand of upstream, on-ramp $R1$, and on-ramp $R2$.

Table 4: Partial traffic data.

$\sigma(O_U)$	$\sigma(O_D)$	RCRI	Y
0.098089	0.088339	−4.50532	1
0.031236	0.032004	−23.0141	1
0.113061	0.013629	−34.9231	1
0.072684	0.014553	−0.28159	0
0.031923	0.045414	−0.68701	0
0.672758	0.080934	−4.76873	0
...	...	...	...

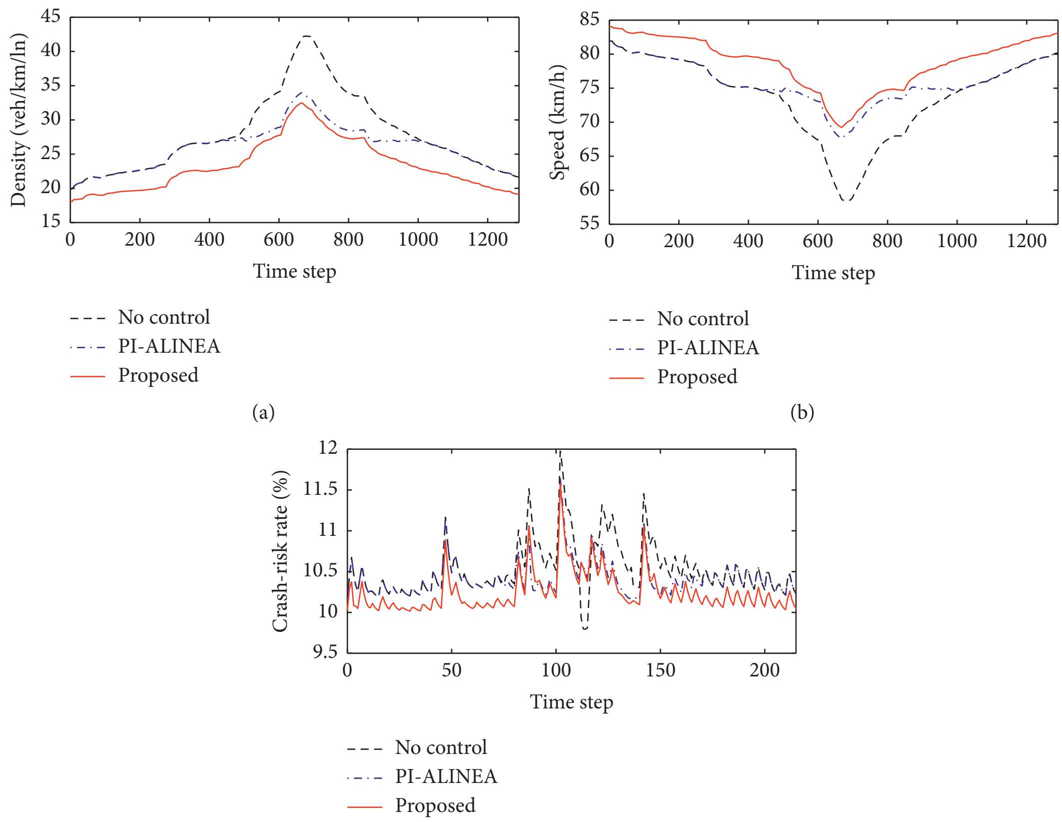

Figure 9: (a) Mainstream density, (b) mainstream speed, and (c) real-time crash-risk probability of different local ramp metering strategies.

physical domains of the density, speed, and visibility of the ramp metering are [32 veh/km/ln, 38 veh/km/ln], [80 km/h, 90 km/h], and [100 m, 200 m], respectively. According to equation (16), the mean values are $\rho_m = 35$ veh/km/h, $v_m = 85$ km/h, and $r_m = 150$ m, and the scaling factors are $K_\rho = 0.2$, $K_v = 0.2$, and $K_r = 0.02$. The parameters in equations (13) and (14) are listed as follows: $K_P = 10$ and $K_R = 40$.

4.2.2. Simulation Results and Analysis. According to equations (20)–(27), a real-time crash-risk prediction model reflecting traffic safety is used to evaluate the proposed local ramp metering. The data on traffic incidents are obtained through a simulation in VISSIM. The location of a traffic incident is shown in Figure 3. The time interval is $\Delta t = 10$ s, the time period is $\Delta T = 60$ s, and $N_1 = \Delta T/\Delta t = 6$ is applied. The real-time crash-risk probability is calculated during every six simulation time steps. The parameters in equation (27) are obtained through the logistic regression of the traffic incident data as follows: $\alpha_1 = -2.2028$, $\alpha_2 = -0.035$, $\alpha_3 = 10.4302$, and $\alpha_4 = 13.3114$. Partial traffic data used for the parameter fitting are listed in Table 4.

The freeway traffic density and speed under different local ramp metering strategies are shown in Figures 9(a) and 9(b), respectively. Equation (27) shows the real-time collision rate, which is used to evaluate the proposed local ramp metering strategy. The real-time collision rate of different local ramp metering strategies is shown in Figure 9(c).

As shown in Figure 9, within the first 500 time steps and the last 260 time steps during the simulation time, the strategies of no-control and PI-ALINEA have similar control results under the traffic state and real-time crash-risk

Table 5: Partial real-time collision rate of different strategies.

No.	PI-ALINEA	Proposed
1	0.101575	0.100297
2	0.104457	0.102950
3	0.106739	0.103447
4	0.104717	0.100847
5	0.103336	0.100757
6	0.102541	0.100483
7	0.104219	0.102161
8	0.105752	0.103796
...	...	...

probability. Because the mainstream density of a freeway is always lower than the desired density, the flow of on-ramp $R2$ is not controlled by PI-ALINEA. As the freeway mainstream density gradually exceeds the desired density, PI-ALINEA will reduce the entrance flow of on-ramp $R2$ and slow down the increasing trend of density to maintain the mainstream density around its critical value at the cost of increasing the ramp queue. Correspondingly, the real-time crash-risk probability will decrease during this period.

As indicated in Figure 9, the proposed ramp metering strategy under foggy weather conditions differs from the PI-ALINEA strategy, which has a consistent effect on on-ramp $R2$. At the beginning of the simulation, on-ramp $R2$ is continuously controlled by the proposed ramp metering strategy under the premise of reducing the real-time crash-risk probability. As shown in Figures 9(a) and 9(b), the fluctuations of the mainstream density and speed are smaller than those controlled by PI-ALINEA. As shown in Figure 9(c), the real-time crash-risk probability of the proposed ramp metering strategy is always lower than that controlled by PI-ALINEA during the entire simulation time step.

In order to further analyze the effects of PI-ALINEA and the proposed strategy, the experimental results of PI-ALINEA and the proposed strategy are used for statistical study. Because the real-time collision rate of different strategies characterizes normal distribution, the t-test is used to evaluate statistical significance with MATLAB. The significant difference between these results is characterized by a significance threshold fixed at a p value less than or equal to 0.05. The calculated p value is much less than 0.01; therefore, the proposed strategy is superior to PI-ALINEA in ensuring traffic safety. Partial experimental data used to evaluate statistical significance are listed in Table 5. On the whole, the proposed ramp metering strategy achieves a better performance in ensuring traffic safety and is more suitable for a freeway system under foggy weather conditions.

5. Conclusions

A macroscopic traffic model applied under foggy weather conditions and based on a model correction factor (c_m) was proposed in this paper. The model correction factor (c_m) is regulated online based on different visibility conditions and curve radius of the freeway to better optimize the traffic model under foggy weather conditions. The sum of the mean absolute percentage error of the mainstream density and speed is used as the fitness function to evaluate the proposed traffic model. A local ramp metering strategy under foggy weather conditions based on the density correction factor (c_d) is proposed when considering the proposed traffic model. The density correction factor (c_d) is regulated online based on the mainstream traffic density, speed, and visibility. A real-time crash-risk prediction model that reflects the level of traffic safety is used to evaluate the performance of the proposed local ramp metering strategy. The simulation results show the effectiveness of the proposed traffic model and ramp metering strategy under foggy weather conditions.

Data Availability

The (Excel) data used to support the findings of this study are included within the supplementary information files.

Conflicts of Interest

The authors declare that there are no conflicts of interest regarding the publication of this paper.

Supplementary Materials

Data 1: data derived from VISSIM by simulating the traffic incident, which are used for parameter regulation in the real-time crash-risk prediction model. These data are complete part corresponding to Table 4 in the manuscript. data 2: data on the real-time collision rate of PI-ALINEA and the proposed strategy, which are used for statistical study. These data are complete part corresponding to Table 5 in the manuscript. (*Supplementary Materials*)

References

[1] K. C. Dey, A. Mishra, and M. Chowdhury, "Potential of intelligent transportation systems in mitigating adverse weather impacts on road mobility: a review," *IEEE Transactions on Intelligent Transportation Systems*, vol. 16, no. 3, pp. 1107–1119, 2015.

[2] S. Choi and C. Oh, "Proactive strategy for variable speed limit operations on freeways under foggy weather conditions," *Transportation Research Record: Journal of the Transportation Research Board*, vol. 2551, no. 1, pp. 29–36, 2016.

[3] P. A. Pisano and L. C. Goodwin, "Research needs for weather-responsive traffic management," *Transportation Research Record: Journal of the Transportation Research Board*, vol. 1867, no. 1, pp. 127–131, 2004.

[4] T. H. Maze, M. Agarwai, and G. Burchett, "Whether weather matters to traffic demand, traffic safety, and traffic operations and flow," *Transportation Research Record: Journal of the Transportation Research Board*, vol. 1948, no. 1, pp. 170–176, 2006.

[5] L. Chris, B. Hellinga, and F. Saccomanno, "Evaluation of variable speed limits to improve traffic safety," *Transportation Research Part C: Emerging Technologies*, vol. 14, no. 3, pp. 213–228, 2006.

[6] B. Ran, P. J. Jin, D. Boyce, T. Z. Qiu, and Y. Cheng, "Perspectives on future transportation research: impact of intelligent transportation system technologies on next

generation transportation modelling," *Journal of Intelligent Transportation Systems*, vol. 16, no. 4, pp. 226–242, 2012.

[7] M. Cools, E. Moons, and G. Wets, "Assessing the impact of weather on traffic intensity," *Weather, Climate, and Society*, vol. 2, no. 1, pp. 60–68, 2010.

[8] M. Abdel-Aty, J. Dilmore, and L. Hsia, "Applying variable speed limits and the potential for crash migration," *Transportation Research Record: Journal of the Transportation Research Board*, vol. 1953, no. 1, pp. 21–30, 2006.

[9] C. Lee, B. Hellinga, and F. Saccomanno, "Assessing safety benefits of variable speed limits," *Transportation Research Record: Journal of the Transportation Research Board*, vol. 1897, no. 1, pp. 183–190, 2004.

[10] M. Papageorgiou and A. Kotsialos, "Freeway ramp metering: an overview," *IEEE Transactions on Intelligent Transportation Systems*, vol. 3, no. 4, pp. 271–281, 2003.

[11] M. Papageorgiou, H. Hadj-Salem, and J. M. Blosseville, "ALINEA: a local feedback control law for on-ramp metering," *Transportation Research Record*, vol. 1320, pp. 58–64, 1991.

[12] E. Smaragdis, M. Papageorgiou, and E. Kosmatopoulos, "A flow-maximizing adaptive local ramp metering strategy," *Transportation Research Part B: Methodological*, vol. 38, no. 3, pp. 251–270, 2004.

[13] Y. Wang, E. B. Kosmatopoulos, M. Papageorgiou, and I. Papamichail, "Local ramp metering in the presence of a distant downstream bottleneck: theoretical analysis and simulation study," *IEEE Transactions on Intelligent Transportation Systems*, vol. 15, no. 5, pp. 2024–2039, 2014.

[14] Z. Hou, J.-X. Xu, and J. Yan, "An iterative learning approach for density control of freeway traffic flow via ramp metering," *Transportation Research Part C: Emerging Technologies*, vol. 16, no. 1, pp. 71–97, 2008.

[15] R. Chi, M. Li, Z. Hou, X. Liu, and Z. Yu, "Freeway traffic density and on-ramp queue control via ILC approach," *Mathematical Problems in Engineering*, vol. 2014, Article ID 321934, 8 pages, 2014.

[16] Z. Hou, J. Yan, J.-X. Xu, and Z. Li, "Modified iterative-learning-control-based ramp metering strategies for freeway traffic control with iteration-dependent factors," *IEEE Transactions on Intelligent Transportation Systems*, vol. 13, no. 2, pp. 606–618, 2012.

[17] H. M. Zhang and S. G. Ritchie, "Freeway ramp metering using artificial neural networks," *Transportation Research Part C: Emerging Technologies*, vol. 5, no. 5, pp. 273–286, 1997.

[18] C. Lu and J. Huang, "A self-learning system for local ramp metering with queue management," *Transportation Planning and Technology*, vol. 40, no. 2, pp. 182–198, 2017.

[19] M. Hasan, M. Jha, and M. Ben-Akiva, "Evaluation of ramp control algorithms using microscopic traffic simulation," *Transportation Research Part C: Emerging Technologies*, vol. 10, no. 3, pp. 229–256, 2002.

[20] L. L. Chen, A. D. May, and D. M. Auslander, "Freeway ramp control using fuzzy set theory for inexact reasoning," *Transportation Research Part A: General*, vol. 24, no. 1, pp. 15–25, 1990.

[21] J. Xu, X. Zhao, and D. Srinivasan, "On optimal freeway local ramp metering using fuzzy logic control with particle swarm optimisation," *IET Intelligent Transport Systems*, vol. 7, no. 1, pp. 95–104, 2013.

[22] A. Ghods, A. Kian, and M. Tabibi, "Adaptive freeway ramp metering and variable speed limit control: a genetic-fuzzy approach," *IEEE Intelligent Transportation Systems Magazine*, vol. 1, no. 1, pp. 27–36, 2009.

[23] X. F. Yu, F. Alam, and W. L. Xu, "Genetic-fuzzy logic ramp metering control for ramp metering of motorway," *International Journal of Computer Applications in Technology*, vol. 50, no. 1/2, p. 30, 2014.

[24] T.-C. Chiang and W.-J. Wang, "Highway on-ramp control using fuzzy decision making," *Journal of Vibration and Control*, vol. 17, no. 2, pp. 205–213, 2011.

[25] H. J. Payne, "FREFLO: a macroscopic simulation model for freeway traffic," *Transportation Research Record*, vol. 722, pp. 68–77, 1979.

[26] W. Z. Qiao, W. P. Zhuang, T. H. Heng, and S. S. Shan, "A rule self-regulating fuzzy controller," *Fuzzy Sets and Systems*, vol. 47, no. 1, pp. 13–21, 1992.

[27] M. R. Bonyadi and Z. Michalewicz, "Particle swarm optimization for single objective continuous space problems: a review," *Evolutionary Computation*, vol. 25, no. 1, pp. 1–54, 2017.

[28] I. C. Trelea, "The particle swarm optimization algorithm: convergence analysis and parameter selection," *Information Processing Letters*, vol. 85, no. 6, pp. 317–325, 2003.

[29] Z. Li, S. Ahn, K. Chung, D. R. Ragland, W. Wang, and J. W. Yu, "Surrogate safety measure for evaluating rear-end collision risk related to kinematic waves near freeway recurrent bottlenecks," *Accident Analysis & Prevention*, vol. 64, pp. 52–61, 2014.